COMMUNICATION

Check for updates

Oscillatory structural forces between charged interfaces in solutions of oppositely charged polyelectrolytes†

Katarzyna Kubiak, Plinio Maroni, Gregor Trefalt (ID) and Michal Borkovec (ID) *

Forces between negatively charged micron-sized silica particles were measured in aqueous solutions of cationic polyelectrolytes with an atomic force microscope (AFM). In these oppositely charged systems, damped oscillatory force profiles were systematically observed in systems at higher polyelectrolyte concentrations, typically around few g L^{-1}. The wavelength of these oscillations is decreasing with increasing concentration. When the wavelength and concentration are normalized with the cross-over concentration, universal power-law dependence is found. Thereby, the corresponding scaling exponent changes from 1/3 in the dilute regime to 1/2 in the semi-dilute regime. This dependence is the same as in the like-charged systems, which were described in the literature earlier. This common behavior suggests that these oscillatory forces are related to the structuring of the polyelectrolyte solutions. The reason that the oppositely charged systems behave similarly to like-charged ones is that the former systems undergo a charge reversal due to the adsorption of the polyelectrolytes to the oppositely charged surface, whereby sufficiently homogeneous adsorbed layers are being formed. The main finding of the present study is that at higher polyelectrolyte concentrations such oscillatory forces are the rule, including the oppositely charged ones.

Small angle neutron and X-ray scattering experiments on polyelectrolyte solutions systematically reveal a structural peak, which indicate the presence of ordered structures.[1–6] The position of this peak suggests that the underlying length scales, at which this ordering occurs, are comparable to (or larger than) the size of individual polyelectrolyte coils. This feature signals the occurrence of a supra-molecular liquid-like structuring in the polyelectrolyte solution. The respective length scale, which typically is a few tens of nanometers, shows a characteristic dependence as $c^{-1/3}$, where c is the polyelectrolyte

Department of Inorganic and Analytical Chemistry, University of Geneva, Sciences II, 30 Quai Ernest-Ansermet, 1205 Geneva, Switzerland.
E-mail: michal.borkovec@unige.ch

† Electronic supplementary information (ESI) available. See DOI: 10.1039/d0sm01257b

concentration.[4–6] This dependence is caused by the formation of a closed-packed structure. The closed-packed objects are the diffuse ionic clouds forming around the charged coils, which induce a soft and long-ranged repulsion among the individual polyelectrolyte molecules. At higher concentrations, the concentration dependence crosses over to $c^{-1/2}$, which signals the onset of the semi-dilute regime.[3–7] In the latter regime, the polyelectrolyte coils interpenetrate and the ordering originates from the repulsion between individual chain segments.

These findings were independently confirmed with direct force measurements between quasi-planar interfaces, which were mostly carried out using an atomic force microscope (AFM).[4–6,8–13] The measured forces show damped oscillatory behavior, which is caused by the formation of ordered layering near the interface. The respective wavelength reveals the same concentration dependence as the length scale inferred from the scattering peak, suggesting that the underlying ordering has the same origin as in the bulk.[4,6] A common feature of these direct force measurements was that the substrates were chosen to have the same sign of charge as the polyelectrolytes, principally to avoid adsorption of the polyelectrolytes to the substrate. However, a charged substrate also induces the formation of an electric double layer in its neighborhood. The diffuse part of this double layer shows a well-defined thickness and an unusual non-exponential concentration profile, which is caused by strong electrostatic repulsion between the polyelectrolyte and the like-charged substrate.[10] Only when the separation distances exceed the thickness of this layer, do oscillatory structural forces set in.

Given all the attention directed towards the like-charged systems, it is surprising that the question of structural forces in oppositely charged systems was so far never addressed. While several researchers have studied the behavior of polyelectrolytes near oppositely charged substrates, investigations focused almost exclusively on the adsorption of polyelectrolytes, which dominates the behavior of these systems at low polyelectrolyte concentrations.[14–22] This adsorption typically induces a charge

reversal of the substrate, which has major consequences on the interaction forces and stability of colloidal suspensions. At higher concentrations, however, similar oscillatory structural forces might occur as reported in the like-charged systems. These structural forces could be expected for the same reason as in the like-charged system, since the oppositely charged system undergoes a charge reversal. However, they could also be substantially weaker or even non-existent. A possible reason for this difference is that the adsorbed polyelectrolyte layer features patch-charge heterogeneities. Surface roughness is known to reduce the amplitude of the oscillatory structural forces, and the same could apply to patch-charge heterogeneities.[23] Whether similar oscillatory structural forces also occur in the oppositely charged systems as in the like-charged systems is therefore not at all obvious.

Here, we address this question by means of direct force measurements with the AFM between pairs of micron-sized silica particles across aqueous solutions of cationic polyelectrolytes. In this oppositely charged system, the water–silica interface is negatively charged due to the ionization of silanol groups,[24] while the cationic polyelectrolytes are positively charged. Fig. 1 illustrates typical normalized force profiles measured in solutions of poly(L-lysine) (PLL) bromide of a molecular mass of 167 kg mol^{-1}. All solutions are adjusted to pH 4.0 with dilute HCl. Under these conditions, the amine groups are completely ionized and PLL is fully charged.[25,26] The fact that the silica surface is also charged at this pH is obvious from the measured force profile shown in Fig. 1a in the absence

of PLL. The observed soft and repulsive force is caused by the repulsion between two overlapping double-layers, which are only present when the interface is charged. The forces reported in Fig. 1 are normalized to the effective radius $R_{eff} = R/2$ where R is the particle radius. The Derjaguin approximation suggests that this normalized force is proportional to the respective surface free energy. Further experimental details are given in the ESI.†

When PLL is added to the system, the force at longer distances remains soft and repulsive. These features indicate the presence of double-layer forces, but their strength weakens, see Fig. 1a. At shorter distances, however, the force becomes more attractive. The weakening of the repulsive part continues until the concentration of 0.07 mg L^{-1} is reached, where the force becomes purely attractive. As the PLL concentration is being increased further, the soft and repulsive force again sets in, converging to a common force profile near the concentration around 1 mg L^{-1}.

This behavior is characteristic for a system undergoing a charge reversal. In the present case, the charge reversal is caused by the adsorption of the positively charged PLL to the negatively charged silica interface. This adsorption process reverses the diffuse layer potential from negative to positive, thereby passing through a charge neutralization point. As long as the interface is charged, the interactions are dominated by repulsive double-layer forces, which extend over a similar range, since the salt concentration remains about the same. With increasing PLL concentration, the magnitude of these forces decreases below the charge neutralization point, while above this point, their magnitude increases. At the charge neutralization point, the double layer force is absent, and the forces become attractive, due to the presence of van der Waals and patch-charge attractions. At higher concentrations, the double layer forces converge to a common profile, indicating the saturation of the adsorbed PLL layer. This charge-reversal scenario has already been observed by direct force measurements earlier, albeit in different oppositely charged systems, including cationic poly(ethylene imine) or dendritic poly(amido amine) adsorbed on negatively charged sulfate latex particles or glass,[27–29] and anionic poly(styrene sulfonate) adsorbed on positively charged amidine latex particles.[30]

The novel features of the force profiles, which are presented in this communication, occur at substantially higher polyelectrolyte concentrations. When the PLL concentration is being increased further, the magnitude of the double layer force increases too. The latter increase indicates the accumulation of additional positive charges. Furthermore, the double layer force starts to decay very rapidly. At PLL concentrations above 0.3 g L^{-1}, damped oscillatory forces set in. When the PLL concentration is further increased, the amplitude of these oscillations increases, while their wavelength decreases.

As pointed out in the introduction, similar oscillatory forces were observed in like-charged systems, particularly, between two negatively charged silica surfaces across solutions of anionic polyelectrolytes, frequently involving sodium poly(styrene sulfonate) (PSS).[4–6,8–12] However, the results presented here
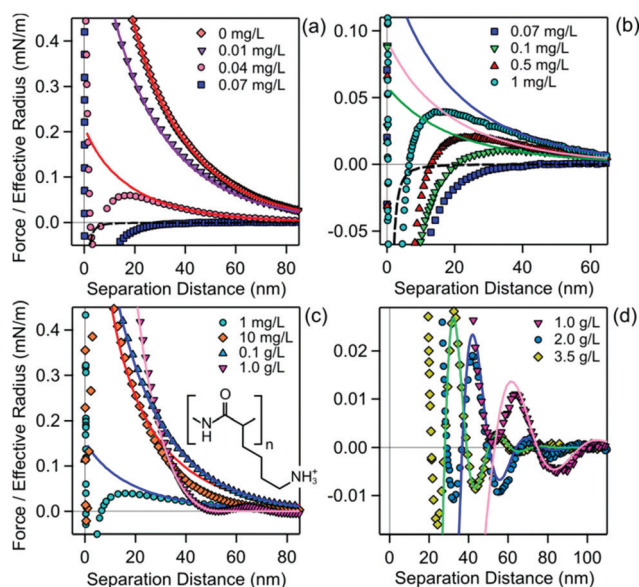
Fig. 1 Forces *versus* separation between silica particles in aqueous solutions at different PLL concentrations at pH 4.0. The PLL concentration increases from (a–d), whereby they are expressed in mg L^{-1} in (a and b) and in g L^{-1} in (c and d). Solid lines are best fits with the PB model (a–c) or damped oscillatory profiles in (d). For the attractive profile, the van der Waals force is indicated as a dashed line in (a and b). (a) Neutralization of the surface charge due to PLL adsorption. (b) Overcompensation of the surface charge. (c) Buildup of strong double-layer repulsion. (d) Onset of oscillatory forces. The structural formula of PLL is given as the inset in (c).

confirm the existence of similar oscillatory forces in an oppositely charged polyelectrolyte system for the first time. In the following, these forces will be analyzed in more detail, and they will be compared to the ones in the like-charged systems. To obtain a more detailed insight concerning the nature of these forces, they were quantified with two different models.

The first model is based on Poisson–Boltzmann (PB) theory, whereby the PB equation was solved numerically. Thereby, the solution is assumed to be composed of monovalent and multi-valent anions, and monovalent cations. The monovalent ions, such as protons and halide ions, originate from the dissociated HCl used to adjust the solution pH and being the counterions of the PLL. For polyelectrolyte concentrations below 0.3 g L^{-1}, the concentration of the counterions originating from the PLL is negligible. Above this concentration, the monovalent ions in the solution are dominated by these counterions, and at the same time, the highly charged PLL ions are present. Within PB theory, this situation is modeled with point ions. Thereby, the polyelectrolyte molecules are represented as multivalent cations with an effective charge Z_{eff}, which are neutralized with monovalent anions. This approach is expected to be applicable at higher concentrations, as the polyelectrolytes are excluded from the vicinity of the interface, and the diffuse layer is dominated by monovalent counterions only. This PB model was recently shown to successfully describe the diffuse layer in the presence of like-charged polyelectrolytes by some of us.[10] Details concerning the PB model and its numerical implementation were published earlier,[31,32] and are also given in the ESI.†

The second model is an exponentially damped oscillatory profile that was proposed to describe the dependence of the structural (or depletion) force F on the separation distance h in hard-sphere and soft-sphere systems at larger distances, namely[33,34]

$$\frac{F}{R_{\text{eff}}} = A e^{-h/\xi} \cos(2\pi h/\lambda + \theta) \qquad (1)$$

where A is the amplitude, ξ is the correlation length, λ is the oscillation wavelength, and θ is the phase shift.

These models were fitted independently to the respective parts of the force curves. The PB model was used at all PLL concentrations. Thereby, the long ranged part of the force profile was fitted below the crossover concentrations. Under these conditions, the PB model was used to extract the diffuse layer potential ψ_{dl} and the regulation parameter p, whereby the concentration of the monovalent electrolyte was fixed to 0.16 mM. These parameters are defined in the ESI.† The fitted regulation parameter fluctuated around a mean of $p = 0.60 \pm 0.13$ where the error bar represents the standard deviation. The force profiles could be successfully fitted by fixing the regulation parameter to the mean value.

At higher concentrations, the profile could be only rationalized with the PB theory at shorter distances, while the oscillatory profile given by eqn (1) must be used at larger distances. Within the PB model, the concentrations of the monovalent salt and of the polyelectrolyte were fixed. The regulation parameter was also fixed to the value determined below the crossover concentration, as the influence of this parameter on the calculated force profiles remains minor. In this fashion, the only adjustable parameters were the diffuse layer potential ψ_{dl} and the effective charge Z_{eff}. Their values could be reliably obtained from the fits. From the oscillatory profiles, all parameters entering eqn (1) could be extracted. The resulting fits are shown as solid lines in Fig. 1 and 2. The latter figure summarizes few selected force curves on a semi-logarithmic scale. This representation allows appreciating the quality of the PB fit over the entire force range.

At low PLL concentrations, the PB theory predicts close to perfectly exponential force curves in full agreement with the experiment down to distances of about 30 nm or less. At smaller distances, attractive forces become important. They are mainly caused by patch charge interactions, and they are much stronger than the van der Waals force, which is also shown as a dashed line in Fig. 1a and b. The latter force is characterized by a Hamaker constant of 1.4×10^{-21} J, which was determined for the same particles in 0.5 M KCl. This value is in good agreement with previous studies[35–37] and the recent theoretical estimate of 1.6×10^{-21} J.[38] These additional
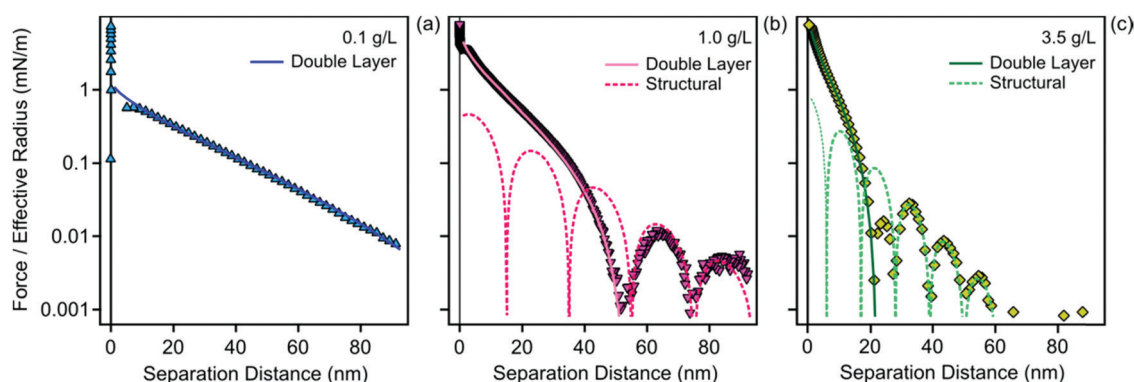

Fig. 2 Semi-logarithmic representation of the absolute value of selected forces profiles shown in Fig. 1. Solid lines are best fits of the double layer forces with the PB model and dotted lines with the damped oscillatory structural force. Note the exponential decay of the double layer force in (a) and the non-exponential one in (b and c). See the caption of Fig. 1 for more details.

short-ranged forces were discussed previously,[22] and will not be analyzed here in detail.

At higher concentrations, the long-ranged part remains exponential up to concentrations of about 0.3 g L^{-1}. This feature is evident in the semi-logarithmic representation shown in Fig. 2a, since the exponential dependence appears as a straight line. Beyond that concentration, oscillatory forces set in and the double-layer force decays in a non-exponential fashion. This non-exponential decay can be easily identified in the semi-logarithmic representation, when comparing Fig. 2b, c with Fig. 2a. Fig. 2 further illustrates that the non-exponential profiles can be well fitted by the PB theory over the entire force range. From these profiles, one can extract an effective charge of the polyelectrolyte Z_{eff} = 180 ± 40, where the error bar represents the standard deviation. This value should be compared with the bare charge of the PLL chain of Z = 800, which can be estimated from the number of ionized groups. The ratio Z_{eff}/Z = 0.23 ± 0.05 agrees quite well with the value of 0.15 ± 0.05, which was obtained in a similar way for poly(styrene sulfonate) (PSS) by Moazzami-Gudarzi et al.[10] The reason that only a small fraction of ions fully dissociate from the polyelectrolyte is the condensation of the remaining ions onto the polyelectrolyte backbone through electrostatic attraction. This phenomenon is referred to as Manning-condensation.[39,40]

In the higher concentration region, oscillatory forces are also present. At larger distances, the oscillatory profiles can be well represented by eqn (1). The transition region between the double layer force and the oscillatory structural force cannot be described by any of the two models. Moreover, the approximation to superpose these two forces, as suggested by Moazzami-Gudarzi et al.[10] leads to poor description of the present data. For this reason, we only focus on the two separate models here.

An important parameter that can be extracted from the PB model is the diffuse layer potential ψ_{dl}. The concentration dependence of this potential is shown in Fig. 3a. Since the sign of the potential cannot be obtained from direct force measurements in such symmetric systems, a negative sign below the

charge neutralization point has been assigned, and a positive one above. This choice is motivated by the known fact that a bare water–silica interface is negatively charged, and that an adsorbing cationic electrolyte will lead to a positively charged interface. The presence of non-exponential double-layer forces occurring at higher PLL concentrations confirms further that the surface is positively charged, see Fig. 2b and c.

To verify the presence of the charge reversal in an independent fashion, electrophoretic mobility measurements have been performed in suspensions of smaller silica particles of pH 4.0 in the presence of PLL. These particles have a diameter of 0.49 μm and these experiments were carried out at a particle concentration of 87 mg L^{-1}. From such measurements, the electrokinetic potentials (ζ-potentials) including their sign can be obtained, see Fig. 3b. One observes that these results show very similar trends to the diffuse layer potentials extracted from force measurements. Note, however, that an equal concentration in the two systems does not reflect the same conditions due to the different surface-to-volume ratio.

At lower concentrations, the diffuse layer potentials show the transition from a negatively charged to positively charged substrate with a charge neutralization point around 0.07 mg L^{-1}. This charge reversal is caused by the adsorption of the cationic PLL to the negatively charged silica surface. At concentrations around 0.10 mg L^{-1} the surface potential reaches a plateau, whereby the surface layer becomes saturated. This plateau is well developed in the electrokinetic potentials, and less so in the diffuse layer potentials. The adsorbed amount of the saturated layer can be estimated from the concentration at the onset of this plateau, as this onset indicates the formation of a saturated layer. The surface-to-volume ratio of the AFM-fluid cell can be related to its thickness of 3.5 mm and the surface coverage by the microparticles within the cell. One then finds about 0.2 ± 0.1 mg m^{-2}, whereby the large error bar mainly originates from the uncertainty concerning the microparticle coverage. A more accurate estimate can be obtained from the onset of an adsorption plateau in the mobility measurements. Thereby, the surface-to-volume ratio can be estimated from the particle concentration and their specific surface area (see the ESI†). One obtains an adsorbed amount of 0.14 ± 0.02 mg m^{-2}, which is in good agreement with the above estimate. These numbers agree well with independent optical reflectivity measurements of the adsorbed mass of PLL on silica substrates under comparable conditions.[19,41] The adsorbed mass per unit area is small, and due to electrostatic attraction the adsorbed polymer film must be thin, most likely below a few nm. This conclusion is in agreement with piezoelectric and dynamic light scattering studies on similar polyelectrolyte systems.[41,42]

At higher PLL concentrations, the surface potential increases beyond the saturation plateau, and this increase continues to the highest concentrations investigated. The onset of this increase is again more pronounced in the electrokinetic potentials, but clearly visible in the diffuse layer potentials too. In this regime, additional PLL adsorbs to the interface, probably leading to a thicker adsorbed film featuring a multilayered
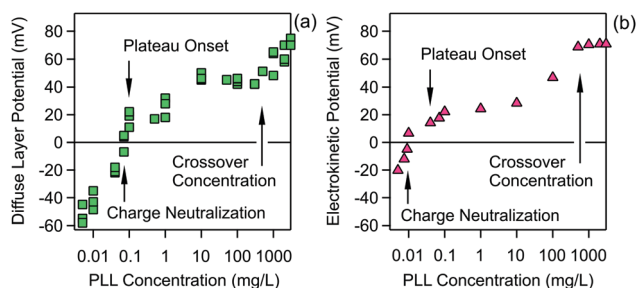

Fig. 3 Surface potentials of silica particles versus the PLL concentration at pH 4.0. (a) Diffuse layer potentials obtained by fitting the measured force profiles with the PB model as shown in Fig. 1 and 2. (b) Electrokinetic potentials obtained from electrophoretic mobilities in suspensions of silica particles of diameter 0.49 μm at a particle concentration of 87 mg L^{-1}. The arrows indicate the charge neutralization point, the adsorption plateau onset, and the crossover concentration.

structure. In any case, when the oscillatory structural forces set in, the surface is very highly charged. While optical reflectivity studies also suggest that the adsorbed amount of PLL also increases with increasing polymer concentration, this increase has been found to be relatively weak.[41] For this reason, we suspect that the pronounced increase in the surface potential shown in Fig. 3 is caused by additional swelling of the adsorbed PLL layer.

Fig. 4 shows the dependence of wavelength λ of the oscillatory forces on the solution concentration c. To compare the present measurements with the existing literature data, the normalized concentration $\tilde{c} = c/c_*$, where c_* is the crossover number concentration, is plotted *versus* the normalized wavelength as $\tilde{\lambda} = \lambda/d$, where d is an effective diameter of the polymer chain defined as $d = c_*^{-1/3}$. This diameter can be interpreted as the distance between nearest neighbor polymers at the crossover concentration. For these normalized variables $\tilde{c}$ and $\tilde{\lambda}$ one may suggest a scaling relation[10,43]

$$\tilde{\lambda} = \tilde{c}^{-\alpha} \qquad (2)$$

where α is the scaling exponent. As discussed further above, one expects the scaling exponents α of 1/3 at low concentrations in the dilute regime, while an exponent of 1/2 at higher concentrations in the semi-dilute regime.[3–7] The prefactor is taken to be one in order to assure that scaling laws with different exponents cross where the normalized variables $\tilde{c}$ and $\tilde{\lambda}$ are unity.

The crossover concentration for the present PLL sample was estimated to be 500 mg L^{-1} by interpolating the previously published viscosity data of salt-free PLL of different molar

Fig. 4 Comparison of the normalized wavelength of the oscillatory force *versus* the normalized polyelectrolyte concentration. The present data for the cationic polyelectrolytes are compared with literature data for various anionic polyelectrolytes.[6,8–10,12,13] The normalization is carried out with the crossover concentration c_* for the concentration $\tilde{c} = c/c_*$ and for the wavelength $\tilde{\lambda} = \lambda/d$, where the apparent diameter d is given by $d = c_*^{-1/3}$. More details about these systems and their crossover concentrations are given in Table S1 in the ESI.†

mass.[44] The effective diameter d obtained from the crossover concentration is 82 nm. This value is comparable to the gyration radius R_g that is accessible by small angle neutron or X-ray scattering. By interpolating the available gyration radii,[45] one obtains the estimate R_g = 50 nm for the present PLL sample, leading to the ratio d/R_g = 1.6. This value is in line with different theoretical estimates, which suggest that this ratio could be anywhere between 1 and 2.[46–48]

The normalized experimental results for the wavelength in the PLL system are shown in Fig. 4 together with the scaling relations given in eqn (2) for the two expected scaling exponents α of 1/3 and 1/2. Fig. 4 further compares the PLL data with available literature data for anionic polyelectrolytes. These like-charged systems include the sodium salts of PSS,[6,10] poly(acrylic acid) (PAA),[12,13] and linear poly(2-acrylamido-2-methylpropanesulfonate) (LPAMPS).[9] These polyelectrolytes are expected to adsorb only weakly, or not at all, since they have the same sign of charge as the silica substrate. The crossover concentrations for PSS were calculated by means of the interpolating function proposed by Lopez.[49] One may again compare the effective diameter d, which is obtained from these crossover concentrations, with the gyration radius R_g, which is known from scattering experiments with PSS solutions.[50] One finds the ratio d/R_g = 1.4, which is independent of the molecular mass. This number is close to our estimate for PLL, and definitely in the range suggested theoretically.[46–48] The crossover concentrations for PAA were taken from Milling *et al.*,[12] while the ones of LPAMPS were estimated from best common scaling. Based on the available gyration radii for PAA,[12,51] which scatter substantially, one finds the ratio d/R_g = 1.5 ± 0.3. This value is still in line with the estimates for other polyelectrolytes quoted above. Table S1 in the ESI† summarizes the data used, together with the corresponding crossover concentrations. The good agreement between the data for the cationic PLL obtained here and the literature data for the anionic polyelectrolytes shown in Fig. 4 suggest the same underlying mechanism for the structuring in all these systems.

The correlation length is comparable to the wavelength. In particular, the ratio λ/ξ is independent of the wavelength, and has a value of about 2.3. The constancy of this ratio indicates that the shape of the force curve is independent of the concentration, and its particular value suggests that several oscillations can be observed in the force profile. The amplitude of the oscillatory force also increases with increasing polymer concentration. These observations are similar to the ones reported for PSS previously.[6,10]

To demonstrate that oscillatory forces are common in other oppositely charged polyelectrolyte systems, two further cationic polyelectrolytes were studied. Fig. 5 shows that oscillatory force profiles can also be observed for poly(2-vinylpyridine) (P2VP) and linear polyethylenimine (LPEI), both with an approximate molecular mass of 245 kg mol^{-1}, in aqueous solutions of pH 3.0. The respective wavelength was extracted by fitting these force profiles with eqn (1). The normalized wavelengths and concentrations shown in Fig. 4 were calculated by finding the best overlap with the remaining data by appropriate choice on
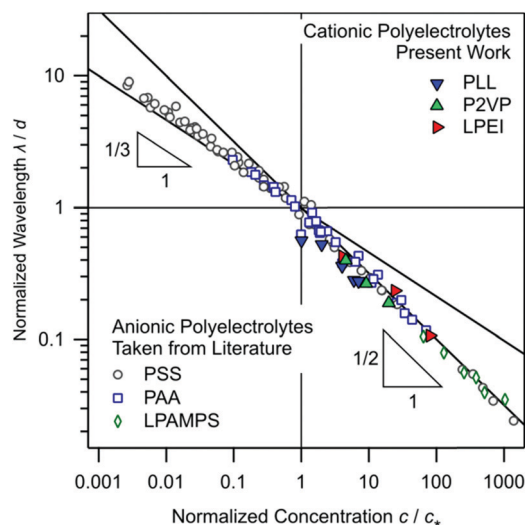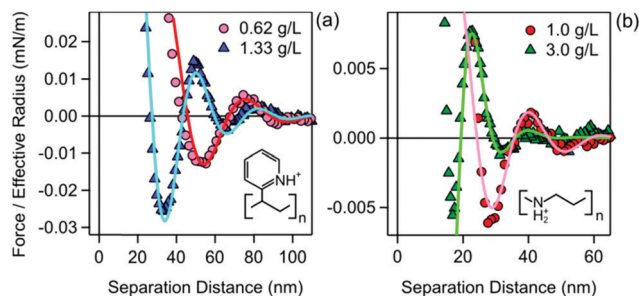
Fig. 5 Oscillatory force profiles measured between negatively charged silica particles in solutions of other oppositely charged polyelectrolytes. (a) P2VP, and (b) LPEI. The insets show the structural formulae of these polyelectrolytes.

an optimal crossover concentration as given in Table S1 (ESI†). This coincidence suggests again that these oscillations originate from the structuring in the polyelectrolyte solutions as in the other systems.

In conclusion, we have observed oscillatory forces between negatively charged silica particles in aqueous solutions of cationic polyelectrolytes. In these oppositely charged systems, these forces typically occur at polyelectrolyte concentrations in the range around few g L^{-1}. When the wavelength and the concentrations are normalized with the cross-over concentration, one finds a universal dependence in all systems, including the like-charged ones, which were described in the literature earlier. This universality strongly suggests that such oscillatory forces are induced by structuring in the polyelectrolyte solutions, and it seems immaterial whether like-charged or oppositely charged systems are being considered.

The presently studied oppositely charged systems also become like-charged, since the surface charge in these systems is reversed due to strong adsorption of the polyelectrolyte. Apparently, the resulting adsorbed layers are sufficiently homogeneous laterally such that the structural order inherent to the polyelectrolyte solutions persists all the way to the surface. While the resulting adsorbed layers have been shown to be inhomogeneous at lower polyelectrolyte concentrations, these inhomogeneities seem to disappear due to additional adsorption and/or swelling of these layers at higher concentrations. The present study thus demonstrates that oscillatory forces between surfaces, which are caused by structuring in polyelectrolyte solutions, are the rule in many polyelectrolyte systems, and this phenomenon is independent of whether the polyelectrolytes are like-charged or oppositely charged with respect to the charge of the substrate.

Conflicts of interest

There are no conflicts of interest to declare.

Acknowledgements

References

1 B. D. Ermi and E. J. Amis, *Macromolecules*, 1998, **31**, 7378–7384.
2 R. Borsali, H. Nguyen and R. Pecora, *Macromolecules*, 1998, **31**, 1548–1555.
3 M. Nierlich, C. E. Williams, F. Boue, J. P. Cotton, M. Daoud, B. Farnoux, G. Jannink, C. Picot, M. Moan, C. Wolff, M. Rinaudo and P. G. D. Gennes, *J. Phys.*, 1979, **40**, 701–704.
4 D. Qu, D. Baigl, C. E. Williams, H. Möhwald and A. Fery, *Macromolecules*, 2003, **36**, 6878–6883.
5 O. Theodoly, J. S. Tan, R. Ober, C. E. Williams and V. Bergeron, *Langmuir*, 2001, **17**, 4910–4918.
6 C. Uzum, S. Christau and R. von Klitzing, *Macromolecules*, 2011, **44**, 7782–7791.
7 M. Drifford and J. P. Dalbiez, *J. Phys. Chem.*, 1984, **88**, 5368–5375.
8 A. J. Milling, *J. Phys. Chem.*, 1996, **100**, 8986–8993.
9 C. Uzum, R. Makuska and R. von Klitzing, *Macromolecules*, 2012, **45**, 3168–3176.
10 M. Moazzami-Gudarzi, T. Kremer, V. Valmacco, P. Maroni, M. Borkovec and G. Trefalt, *Phys. Rev. Lett.*, 2016, **117**, 088001.
11 A. J. Milling and B. Vincent, *J. Chem. Soc., Faraday Trans.*, 1997, **93**, 3179–3183.
12 A. J. Milling and K. Kendall, *Langmuir*, 2000, **16**, 5106–5115.
13 M. Piech and J. Y. Walz, *J. Phys. Chem. B*, 2004, **108**, 9177–9188.
14 J. Gregory, *J. Colloid Interface Sci.*, 1973, **42**, 448–456.
15 N. G. Hoogeveen, C. W. Hoogendam, R. Tuinier and M. A. Cohen Stuart, *Int. J. Polym. Anal. Charact.*, 1995, **1**, 315–328.
16 R. Rehmet and E. Killmann, *Colloids Surf., A*, 1999, **149**, 323–328.
17 I. Popa, B. P. Cahill, P. Maroni, G. Papastavrou and M. Borkovec, *J. Colloid Interface Sci.*, 2007, **309**, 28–35.
18 I. Popa, G. Gillies, G. Papastavrou and M. Borkovec, *J. Phys. Chem. B*, 2009, **113**, 8458–8461.
19 M. Jiang, I. Popa, P. Maroni and M. Borkovec, *Colloids Surf., A*, 2010, **360**, 20–25.
20 I. Szilagyi, D. Rosicka, J. Hierrezuelo and M. Borkovec, *J. Colloid Interface Sci.*, 2011, **360**, 580–585.
21 F. Xie, T. Nylander, L. Piculell, S. Utsel, L. Wagberg, T. Akesson and J. Forsman, *Langmuir*, 2013, **29**, 12421–12431.
22 I. Szilagyi, G. Trefalt, A. Tiraferri and M. Borkovec, *Soft Matter*, 2014, **10**, 2479–2502.
23 Y. Zeng and R. von Klitzing, *Langmuir*, 2012, **28**, 6313–6321.
24 M. Kobayashi, M. Skarba, P. Galletto, D. Cakara and M. Borkovec, *J. Colloid Interface Sci.*, 2005, **292**, 139–147.
25 P. Appel and J. T. Yang, *Biochemistry*, 1965, **4**, 1244–1249.
26 Y. N. Vorobjev, H. A. Scheraga and B. Honig, *J. Phys. Chem.*, 1995, **99**, 7180–7187.
27 E. Poptoshev and P. M. Claesson, *Langmuir*, 2002, **18**, 2590–2594.
28 M. Finessi, P. Sinha, I. Szilagyi, I. Popa, P. Maroni and M. Borkovec, *J. Phys. Chem. B*, 2011, **115**, 9098–9105.
29 I. Popa, G. Papastavrou and M. Borkovec, *Phys. Chem. Chem. Phys.*, 2010, **12**, 4863–4871.

30 I. Popa, G. Gillies, G. Papastavrou and M. Borkovec, *J. Phys. Chem. B*, 2010, **114**, 3170–3177.

31 W. B. Russel, D. A. Saville and W. R. Schowalter, *Colloidal Dispersions*, Cambridge University Press, Cambridge, 1989.

32 G. Trefalt, I. Szilagyi and M. Borkovec, *J. Colloid Interface Sci.*, 2013, **406**, 111–120.

33 S. H. L. Klapp, Y. Zeng, D. Qu and R. von Klitzing, *Phys. Rev. Lett.*, 2008, **100**, 118303.

34 A. Trokhymchuk, D. Henderson, A. Nikolov and D. T. Wasan, *Langmuir*, 2001, **17**, 4940–4947.

35 A. M. Smith, P. Maroni, G. Trefalt and M. Borkovec, *J. Phys. Chem. B*, 2019, **123**, 1733–1740.

36 M. Dishon, O. Zohar and U. Sivan, *Langmuir*, 2009, **25**, 2831–2836.

37 V. Valmacco, M. Elzbieciak-Wodka, C. Besnard, P. Maroni, G. Trefalt and M. Borkovec, *Nanoscale Horiz.*, 2016, **1**, 325–330.

38 H. D. Ackler, R. H. French and Y. M. Chiang, *J. Colloid Interface Sci.*, 1996, **179**, 460–469.

39 G. S. Manning, *J. Chem. Phys.*, 1969, **51**, 924–933.

40 E. Trizac and G. Tellez, *Phys. Rev. Lett.*, 2006, **96**, 038302.

41 M. Porus, P. Maroni and M. Borkovec, *Langmuir*, 2012, **28**, 5642–5651.

42 E. Seyrek, J. Hierrezuelo, A. Sadeghpour, I. Szilagyi and M. Borkovec, *Phys. Chem. Chem. Phys.*, 2011, **13**, 12716–12719.

43 Y. Zeng, S. Grandner, C. L. P. Oliveira, A. F. Thunemann, O. Paris, J. S. Pedersen, S. H. L. Klapp and R. von Klitzing, *Soft Matter*, 2011, **7**, 10899–10909.

44 E. C. Cooper, P. Johnson and A. M. Donald, *Macromolecules*, 1991, **24**, 5380–5386.

45 O. A. Nehme, P. Johnson and A. M. Donald, *Macromolecules*, 1989, **22**, 4326–4333.

46 G. C. Berry, H. Nakayasu and T. G. Fox, *J. Polym. Sci., Polym. Phys. Ed.*, 1979, **17**, 1825–1844.

47 W. W. Graessley, *Polymer*, 1980, **21**, 258–262.

48 Q. C. Ying and B. Chu, *Macromolecules*, 1987, **20**, 362–366.

49 C. G. Lopez, *Macromolecules*, 2019, **52**, 9409–9415.

50 C. G. Lopez and W. Richtering, *J. Chem. Phys.*, 2018, 148.

51 R. Schweins, P. Lindner and K. Huber, *Macromolecules*, 2003, **36**, 9564–9573.